Density Profiles of Simulated Combburst Molecules

Robert L. Lescanec and M. Muthukumar*

Polymer Science and Engineering Department, University of Massachusetts, Amherst, Massachusetts 01003

Received October 3, 1990; Revised Manuscript Received April 10, 1991

ABSTRACT: The growth behavior and resulting intramolecular characteristics of combburst systems are simulated by using the kinetic self-avoiding-walk algorithm. Simulated combburst molecules characterized by T (=2–5) teeth and flexible spacers of P (=2–6) steps are compared to starburst analogues. Intramolecular radial density distributions from the center of mass of the combburst molecule as a function of P exhibit a characteristic "core" region appearing immediately, delineating two regimes of growth. This is in contrast to their starburst analogues, where the core region is not seen until the third generation. Generally, the density distributions for all (T,P) indicate that the branches of the combbursts are highly folded, spanning the entire molecule throughout growth. The ensemble-averaged radius of gyration, R_g, of the molecule is characterized by $R_g \sim M^{\rho}P^{\nu}$ throughout growth for all T. The apparent size exponents ρ and ν change throughout growth with $\rho = 0.22 \pm 0.05$ and $\nu = 0.50 \pm 0.05$ at high molecular weights, providing evidence of transitional growth resulting from the *modified Cayley tree* branching nature of starburstlike systems.

Introduction

Recently, a particular class of starlike polymers—starburst dendrimers—has received much attention due to the development of controlled, stepwise synthetic routes, yielding successive generations of dendrimers.[1-3] Characterization of their structurally dependent physical properties[3,4] followed, providing insight into their branch growth behavior and resulting molecular dimensions. Fueling this interest is the potential utility of these molecules as transport media for catalytic agents due to their predicted "host–guest" nature.[5]

Following their first synthesis, theoretical investigation[6] analytically predicted molecular dimensions, limits of growth, and intramolecular configurational details of starburst molecules in an attempt to provide a fundamental explanation of their observed physical phenomena. In the same spirit, simulation techniques[7,8] were employed to further describe the mechanisms governing growth and resulting physical behavior of starburst molecules.

Prior to the synthesis of the first dendrimer, the underlying branching process governing starburst growth, Cayley tree branching, was the repeated topic of theoretical investigation. The percolative behavior[9,10] of the Cayley tree, or Bethe lattice, was intensively studied as a model structure to describe various critical phenomena[11] including polymer gelation.[12-14] We have shown[8] that the Cayley tree is also suitable as a conceptual model for high molecular weight starburst molecules simulated under specific conditions.

A novel modification of starburst branching, resulting in a form equally rich in structural detail, is the topic of study here. These systems will be termed *combbursts*. Combburst and starburst systems will share the same fundamental growth process but differ with respect to connectivity. Combbursts will have chains originating from junctions uniformly spaced along the contour of a chain, in contrast to starburst molecules whose branches emanate from a single junction. Thus, this combburst model is a logical extension of the starburst structure.

Although synthesized combbursts have not been reported in the literature to the best of our knowledge, the technology developed to perform the stepwise procedure necessary to grow starburst molecules appears to be a viable method, with modification, to make combburst polymers. Since the same branching process is intrinsic to both combburst and starburst molecules, these two molecular classes are expected to demonstrate similar physical behavior and be of comparable utility as host–guest media.

In our previous work,[8] we presented a kinetic model to simulate the growth of starburst molecules. This method is now extended to study the growth behavior and resulting configurational characteristics of combburst molecules. The "seed" combs generated in this study, the basis for the individual combs forming the combburst, have two, three, four, and five teeth separated by flexible spacers of different lengths (i.e., variable branch density). The simulation algorithm grows all branches of the same generation simultaneously. The number of teeth and spacer lengths considered here will yield combburst molecules of comparable molecular weight to starburst analogues grown from an ideal synthesis.[1,2]

With the number of teeth and spacer length as the primary parameters describing combbursts, the intramolecular radial density distribution from the center of mass, the ensemble-averaged radius of gyration of the molecule, tooth (branch) end-to-end distances, and growth statistics are calculated as each generation is grown.

The configurational properties of comb polymers (first generation combburst molecules) have been rigorously investigated by several methods. Self-consistent analytical techniques[15] were employed to predict the dimensions of the component branches of combs as a function of branch density. Exact enumeration techniques and Monte Carlo simulations[16] provided a description of the scaling behavior of combs having two branch points of varying functionality. In contrast to these studies, the primary goal in this study is to provide *qualitative* insight into the mechanisms governing the physical behavior of ideally synthesized high molecular weight combbursts.

Model and Simulation Technique

The combburst molecules here are modeled by using conditions to mimic a dilute, "good" solution environment. These conditions are selected to determine if excluded volume interactions are influencing chain flexibility and molecular dimensions. Branch density (i.e., the number of branches per backbone bead), in the form of two variables (see below), is the characteristic parameter of the simulation.

Parts a–c of Figure 1 show a bead–stick representation of the growth and connectivity of a typical combburst molecule through two generations. In this study, comb-

0024-9297/91/2224-4892$02.50/0

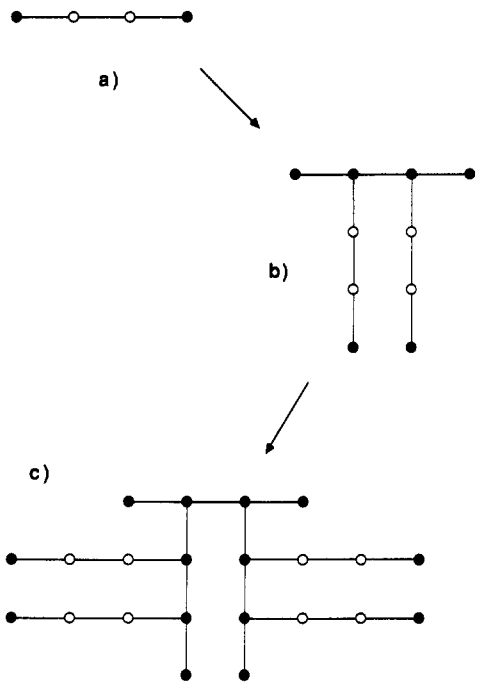

Figure 1. Illustration of combburst growth and connectivity through (a) zero, (b) one, and (c) two generations of growth for $T = 2$ teeth and a spacer length of $P = 1$ step.

burst systems are classified based on the number of teeth, T, and the spacer length, P, characteristic of the "seed" comb, formed upon completion of the first generation (part b of Figure 1). Thus, the system pictured here has $T = 2$ teeth and a spacer length of $P = 1$ segment between beads. In combburst growth, the teeth generated in generation N will be the backbones for the teeth formed upon the completion of generation $N + 1$. For clarity, the beads of generation N that will serve as branch points for tooth formation in generation $N + 1$ are unshaded (○) in Figure 1.

The stepwise development of a combburst molecule begins with the growth of a linear chain (part a of Figure 1), which will serve as the backbone for the comb formed in the first generation of growth. The molecular weight of this backbone, M_0 (and all subsequent "teeth" generated), is determined by the number of teeth and the spacer length desired with $M_0 = P(T + 1) + 1$. Upon completion of the "generation 0" backbone, the teeth of generation 1 grow simultaneously from the indicated branch points (part b of Figure 1) and will become the backbones for the teeth generated in generation 2 (part c of Figure 1). The molecular weight of a combburst molecule, growing exponentially with generation, is described at any generation, G, by

$$M_G = \frac{T^{G+1} - 1}{T - 1}(M_0 - 1) + 1 \qquad (1)$$

The algorithm employed to grow the combburst molecules in this study is the kinetic self-avoiding walk (KSAW).[17] The reader is referred to our previous work and the references contained therein as to the details regarding the implementation of this algorithm in a three-dimensional off-lattice stepwise synthesis. The KSAW algorithm was selected for these studies due to its ease in growing highly branched, high molecular weight systems. Implementing the traditional relaxation algorithms such as kink-jump[18,19] or reptation[20] to simulate such systems would prove excessively time consuming with the current computational technology.

In the KSAW scheme, growth of the molecule ceases when *any* branch end becomes frustrated, that is, when no additional beads may be added to that particular branch due to excluded volume arising from beads already present. Note that since growth of a molecule terminates due to a single instance of branch-end frustration, other branches of that generation may not have frustrated ends and therefore are still capable of growth. Furthermore, when employing this kinetic growth algorithm, no dynamics are used to relieve branch-end frustration occurring during growth or after growth termination of a combburst molecule.

After growth termination, the molecule is truncated to the last completed generation and constitutes a statistical sample. For each sample generated, the radial density distribution from the center of mass, the mean-squared radius of gyration of the molecule, and the mean-squared end-to-end tooth (branch) length are calculated for each completed generation. Also, the average growth of a combburst molecule at a specified T and P is noted. The radial density distribution (with density expressed as a volume fraction) is calculated by dividing space into spherical shells centered around the center of mass of the molecule and counting the number of beads in each shell. The volume fraction, ϕ, at a given radial distance from the center of mass, $|r - r_{cm}|$, is the total volume of spherical beads in the shell divided by the volume of the shell. The mean-squared radius of gyration and the mean-squared end-to-end tooth length are calculated in the manner outlined by Zimm and Stockmayer.[9] The error in all quantities reported here is ±10% unless otherwise indicated.

In this study, we investigate combburst molecules having simulation parameters of $T = 2$–5 teeth and spacer lengths of $P = 2$–6 steps between branch points in the seed comb. Here we note that as P is varied, each stick connecting *any* two beads in Figure 1 is modeled as a spacer composed of $P - 1$ beads of diameter $d = 1$ (arbitrary units) connected by P Kuhn steps[21] of length $l = 1.2$. These values of d and l are selected to prevent bond crossing, which cannot exist in a physical system. The algorithm makes 5000 attempts to place a bead before terminating growth due to apparent branch-end frustration. For each, (T,P) studied, 5000 statistical samples are evaluated when determining all ensemble averages.

Results and Discussion

The evolution of a typical combburst molecule with $T = 2$ and $P = 3$ generated by the KSAW algorithm is shown in parts a–e of Figure 2. The convention used in shading the beads in Figure 1 is also employed here. Note that the branches of the combburst molecule are highly folded, traversing the entire molecule, at all stages of growth, as were the branches in the analogous kinetically grown starburst structures.

The implementation of the KSAW algorithm to simulate the stepwise growth of starbursts yields polydisperse molecules, with the ensemble having a characteristic molecular weight distribution.[8] Since a distribution of molecular weights is also expected for the kinetically grown combburst molecules, Figure 3 is a plot of the ensemble-averaged molecular weight of the combbursts versus spacer length for two, three, four, and five teeth (branches) on the seed comb. Reasonable collapse of these curves is seen, within error, for the combburst cases. This indicates that chain flexibility and, hence, packing are unaffected by the tooth (branch) density of the combburst molecules throughout all stages of growth. This curve for the starburst case is also included. Note that although the curve

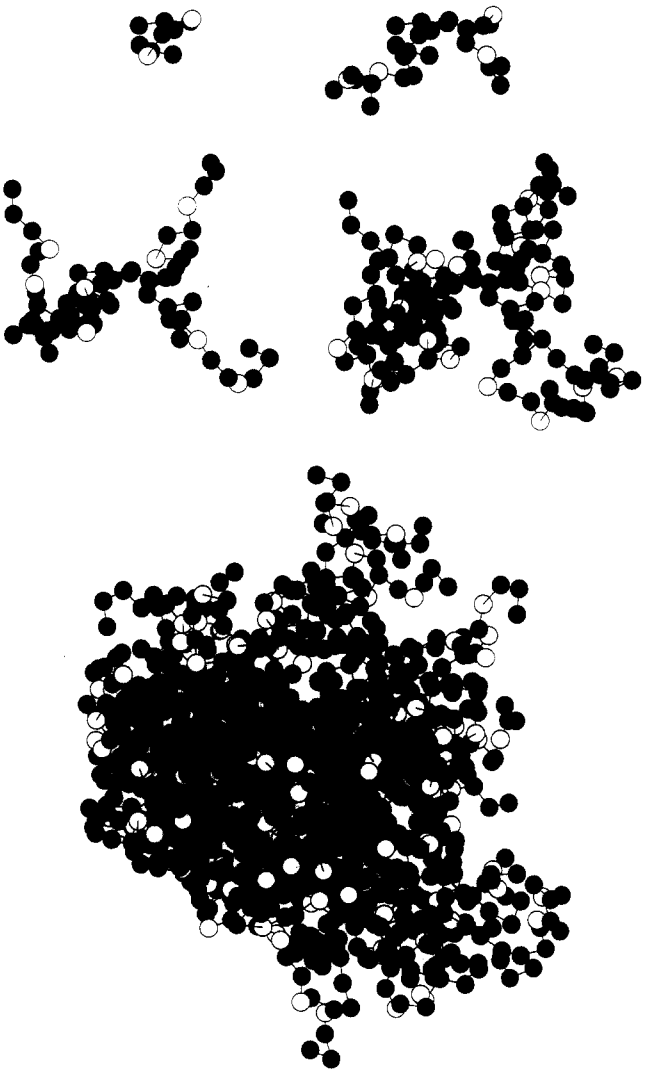

Figure 2. Typical combburst configuration through (a, top left) zero, (b, top right) one (c, middle left) two, (d, middle right), three, and (e, bottom) six generations of growth for $T = 2$ teeth and a spacer length of $P = 3$ steps.

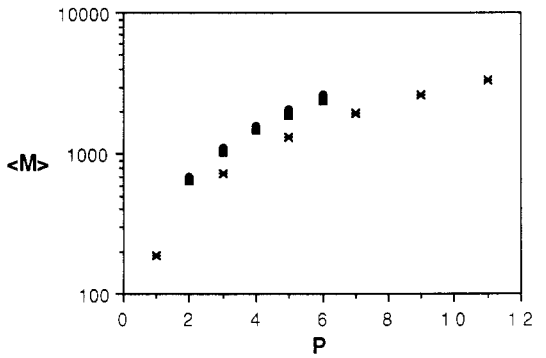

Figure 3. Ensemble-averaged molecular weight, $\langle M \rangle$, versus spacer length, P, for combbursts having two (●), three (■), four (▲), and five (♦) teeth. Note the inclusion of the analogous curve (*) for the starburst case (see text).

is identical in shape with those of the combburst molecules, it lies consistently below them. This results from essential differences in combburst and starburst configurational detail. Branches in any generation of a combburst molecule are uniformly spaced along the contour of a chain, while in starburst molecules they are confined to a branch point. Consequently, when compared to their starburst analogues, combburst molecules maintain a relatively "open" structure during early growth. This facilitates later

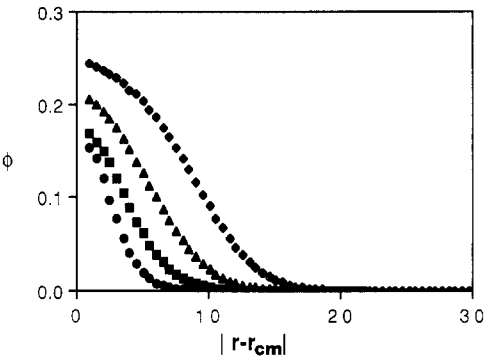

Figure 4. Radical density distributions from the center of mass for combbursts having $T = 3$ and $P = 4$. Here, ϕ is the bead volume fraction at distance $|r - r_{cm}|$ from the center of mass. Growth is shown through one (●), two (■), three (▲), and four (◆) generations.

stage branch penetration into the matrix and allows more efficient packing in combburst molecules than in starbursts throughout growth.

Figure 4 is a density distribution of beads from the center of mass for combburst molecules having $T = 3$ and $P = 4$ through four generations of growth. The shapes and relative locations of these profiles to one another are typical for all T and P investigated here. As seen for starburst molecules, the density of a combburst molecule monotonically decreases outward from its center of mass throughout all stages of growth. Since the density of the molecule increases uniformly at all radial distances from its center of mass, it is evident that the growing branch ends span the combburst molecule throughout all stages of growth.

Parts a–d of Figure 5 show radial density distributions of beads from the center of mass for $T = 3$ and all spacer lengths through four generations of growth.

The predominant feature present in these figures is an inversion, located at r_{inv} and characterized by the volume fraction ϕ_{inv}. r_{inv} as well as ϕ_{inv} is seen to increase monotonically with generation. This behavior is general for all (T,P) investigated here. The presence of this inversion is seen to delineate two types of growth behavior. This is qualitatively understood through the emergence of a "core" region.[8] The first type is seen in the region bounded by $|r - r_{cm}| < r_{inv}$. In this core region, the density of the molecule *decreases* with *increasing* spacer length at any radial distance from the center of mass. Combburst molecules having shorter branches will initially form more "porous" cores than those with longer branches (larger P), allowing for frequent branch interpenetration during late stage growth. Consequently, combburst molecules having shorter spacers will more effectively contribute molecular density to the core.

The second type of growth behavior, lying beyond the core region, is a natural result of core formation. Since the branches of combburst molecules having longer spacers have more difficulty penetrating the core, they are more easily reflected outward into the region $|r - r_{cm}| > r_{inv}$, resulting in *increasing* density with *increasing* spacer length at all distances from the center of mass of the molecule.

Note that the core region is formed much earlier in growth for combburst molecules that their respective starburst analogues (cf. parts a–d of Figure 5 in ref 8). The presence of a core is seen in combburst molecules at the completion of the first generation, while in starburst molecules the appearance of a core is not seen until the third generation of growth. This is another result of the

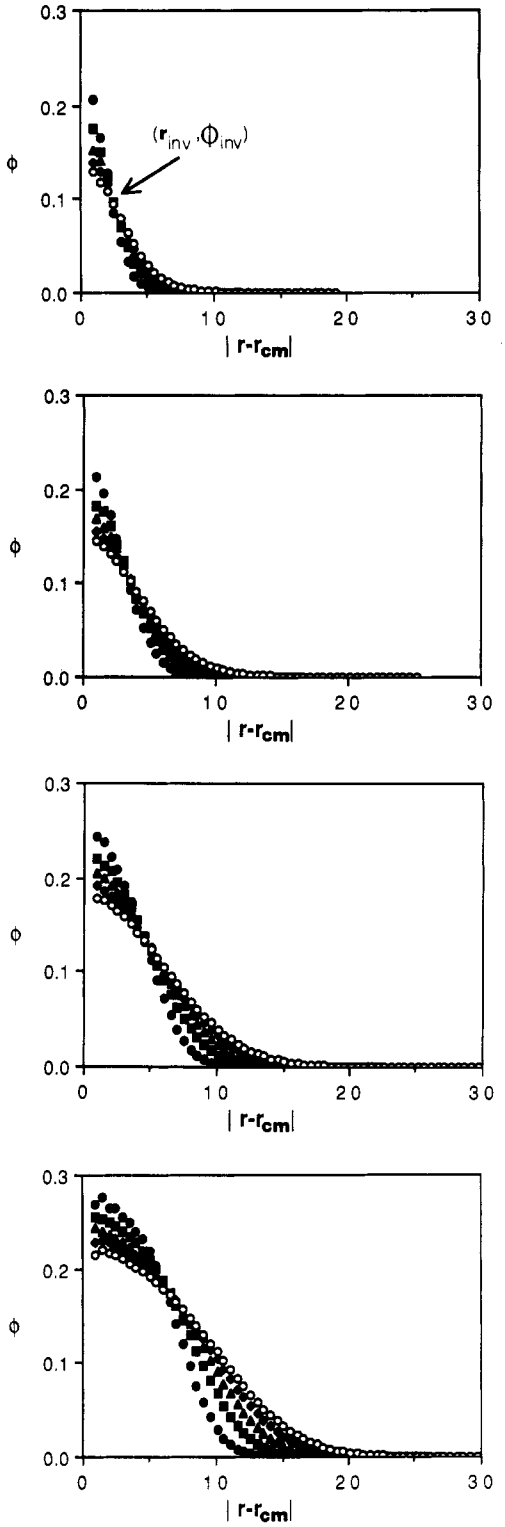

Figure 5. Radial density distributions from the center of mass for $T = 3$ as a function of spacer length at (a, top) one, (b, top middle) two, (c, bottom middle) three, and (d, bottom) four generations. ϕ is the bead volume fraction at a distance $|r - r_{cm}|$ from the center of mass. Spacer lengths of $P = 2$ (●), 3 (■), 4 (▲), 5 (◆), and 6 (○) steps are shown. Note that the location of (r_{inv},ϕ_{inv}) is indicated in part a.

connectivity differences between combburst and starburst molecules, with combburst molecules lacking the center of symmetry characteristic of the starburst structure.

In order to determine the effect of variations in T at constant P on the density profiles, parts a and b of Figure 6 show the radial density distributions from the center of mass for $P = 6$ and $T = 2$–5 through one (part a) and three (part b) generations. At the completion of one generation

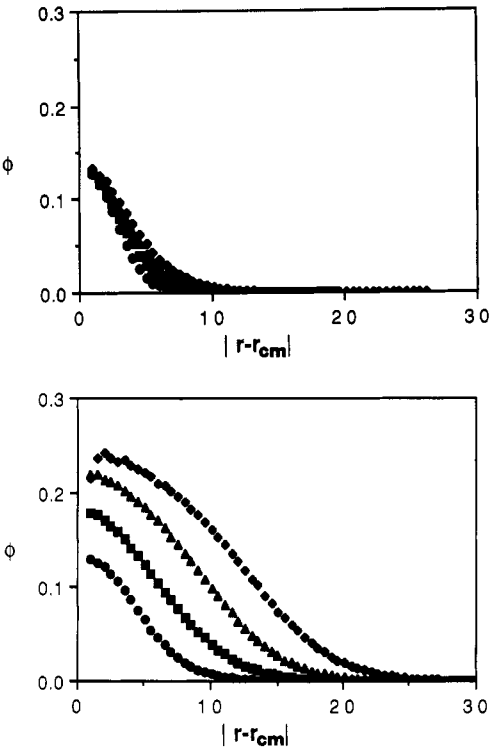

Figure 6. Radial density distributions from the center of mass for $P = 6$ as a function of the number of teeth on the seed comb, T, at (a, top), one and (b, bottom) three generations. ϕ is the bead volume fraction at a distance $|r - r_{cm}|$ from the center of mass. Distributions for $T = 2$ (●), 3 (■), 4 (▲), and 5 (◆) teeth are shown.

of growth, the density at a particular $|r - r_{cm}|$ is seen to increase as T increases. Increasing T at constant P directly increases branch length, and hence, the degree of branch folding increases. This increase in branch folding allows a more effective contribution of molecular density to all shells of the distribution. One notes, however, that the relative increase in ϕ at the inner shells ($|r - r_{cm}| \sim 2d$, for $P = 6$) is much smaller than that for the outer shells of the distribution. This behavior results from the inability of the branches to deeply penetrate the molecule due to the small degree of branching characteristic of the first generation (regular comb polymer). However, by the third generation of growth, the molecule exhibits a more fully developed, highly branch structure. Thus, newly grown branches are able to spread through the molecule, leading to a more uniform contribution of molecular density throughout the profile.

With $\langle R_b \rangle$ and N_0 denoting respectively the average end-to-end distance of the branches and the number of bonds present in the branches (note that $N_0 = M_0 - 1$) of a combburst molecule, Figure 7 is a double-logarithmic plot of $\langle R_b \rangle$ versus N_0. Throughout growth, the dependence of $\langle R_b \rangle$ on N_0 is reasonably characterized by

$$\langle R_b \rangle \sim N_0^{0.57\pm0.05} \tag{2}$$

An *asymptotic* KSAW was shown to have an upper critical dimension, $d_c = 4 - \epsilon$, placing it in the self-avoiding-walk universality class.[22] This suggests that excluded volume interactions may be affecting the exponent, ν, of N_0. Although the apparent size exponent remains invariant of growth, a vertical skew in the data is seen as the molecule grows. This branch stretching results from a radially symmetric intramolecular potential arising from the continuous buildup of the core region mentioned above.

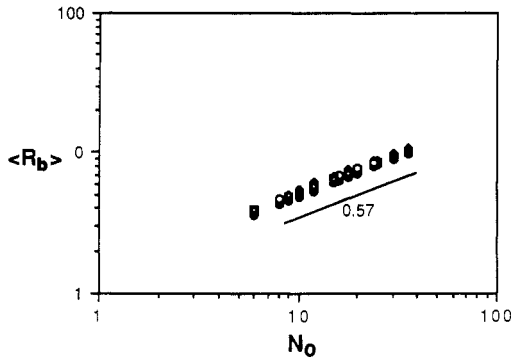

Figure 7. Average branch (tooth) end-to-end distance, $\langle R_b \rangle$, versus number of bonds per branch, N_0, through zero (●), one (■), two (▲), three (◆), four (○), five (□), six (△), and seven (◇) generations of combburst growth.

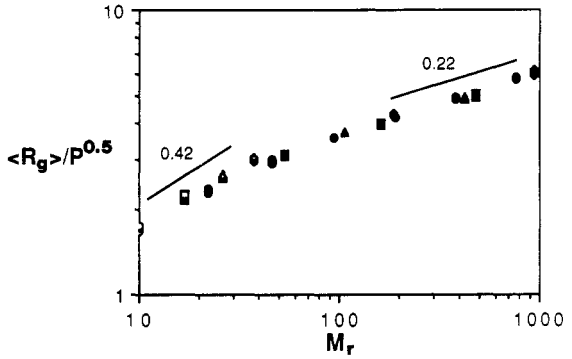

Figure 8. $\langle R_g \rangle / P^{0.5}$ versus reduced molecular weight (see text), M_r, for $T = 2$ (●), 3 (■), 4 (▲), and 5 (◆) teeth. In addition, the data for the first generation combbursts (regular combs) are highlighted for the respective T by analogous unshaded plotting symbols.

Having characterized the branch growth behavior by a power law, it follows that the distance between branches is then proportional to P^{ν}, where $\nu = 0.57 \pm 0.05$. However, due to the degree of uncertainty inherent in these quantities when determined by such a kinetic simulation,[17,22,23] a broader range of this apparent exponent is considered when attempting to characterize combbursts. The range $0.50 < \nu < 0.60$ is explored to determine the degree to which excluded volume interactions influence ν.

Figure 8 is a double-logarithmic plot of the reduced average radius of gyration, $\langle R_g \rangle / P^{\nu}$ with $\nu = 0.50$ versus the reduced molecular weight, M_r. The scale factor, $1/P^{\nu}$, applied to the average radius of gyration facilitates the collapse of the $\langle R_g \rangle$ versus M curves for all P at a particular value of T. In an effort to achieve a collapse of these data for all T, the concept of a reduced molecular weight is utilized. Since the spacers (the solid lines of Figure 1) only provide a length scale for the connected branch points (and the chain ends) of the combs, their molecular weight contribution is recognized when $\langle R_g \rangle$ is scaled. All that remains to be considered are the branch points and chain ends themselves, that is, the minimum number of beads needed to define the combburst architecture for a particular T. This molecular weight is defined to be M_r. Figure 1 shows the beads necessary to determine M_r for the case of $T = 2$ (from eq 1, with $P = 1$: $M_r = 10, 22, 46, \ldots$, for $G = 1, 2, 3, \ldots$, when $T = 2$).

At *high* M_r ($M_r > \sim 100$), the data for *all* T are characterized by a line with slope $\rho = 0.22 \pm 0.05$, indicating an apparent dimensionality, $d_{app} \sim 4$, identical with that of the kinetically grown high molecular weight starburst molecules.[8] Therefore, at high molecular weights, combburst molecules demonstrate the same power law behavior as their starburst analogues; that is,

$$\langle R_g \rangle / P^{0.50} \sim M_r^{0.22 \pm 0.05} \quad (3)$$

This behavior is expected since, along with the independence of d_f (d_{app} here) for Cayley trees on branch functionality,[9,10] the same branching process governs combburst and starburst growth, with a simple analysis yielding $M^c_G = M^s_{G+1}$, where M^c and M^s are the molecular weights of "similar" combburst and starburst systems, respectively. ("Similar" systems have common P with combbursts characterized by T teeth on the seed comb and starburst branch points of functionality $T + 1$.) A length scale of $P^{0.50}$ provides the best collapse of the data at a given T in the high molecular weight region. This length scale indicates that any excluded volume interactions that may be occurring during the early stages of growth are screened due to late generation branch interpretation into the existing matrix of branches.

When a scale factor of $1/P^{0.57}$ is used in the above formalism to collapse the data, one sees results directly contrasting those described above. Using this length scale, the best collapse is seen at *low* combburst molecular weights ($M_r < \sim 100$), where the excluded volume effect may be influencing branch growth due to the low intramolecular density present during the early stages of combburst growth.

Finally, the statistical behavior of regular comb polymers formed during the first generation of combburst growth is investigated. These data are highlighted in Figure 8 for the respective T. The power law best describing these regular combs is

$$\langle R_g \rangle / P^{0.57} \sim M_r^{0.42 \pm 0.05} \quad (4)$$

The factor $1/P^{0.57}$, collapsing the data for all P at a given T, indicates that the conformation of the branches at this stage of growth appears to be influenced to some degree by excluded volume interactions. This is in agreement with analytical results[15] as well as those from Monte Carlo estimates and exact enumeration techniques.[16]

The comb polymers exhibit interesting behavior with respect to variations in reduced molecular weight. The exponent of M_r, $\rho = 0.42 \pm 0.05$, indicates that the short chains comprising the comb show very compact packing. This is a result of the strong interference seen between the branches of comb polymers.[16] These branch–branch interactions, studied in combs having *only* two branch points, were shown to strongly affect scaling law prefactors. Since the combs in this study have T (=2–5) branch points, we expect these interactions to be more severe, affecting not only prefactors but also apparent exponents. Further study on combs having more than two branch points is necessary to fully explore the consequences of branch–branch interference.

Conclusions

The kinetically grown combburst molecules show remarkable similarities to their starburst analogues with respect to intramolecular packing, as seen in the comparative density profiles, and high molecular weight power law behavior indicating $R_g \sim M^{\rho}P^{\nu}$ with $\rho = 0.22 \pm 0.05$ ad $\nu = 0.50 \pm 0.05$ for both types of molecules. The combburst molecules, starting configurationally as regular combs, grow by "modified Cayley tree" branching and exhibit the configurational behavior of kinetically grown starburst molecules.

Although showing many structural similarities, combburst and starburst systems show notable differences

regarding the development of their respective core regions. The presence of a core is immediately seen in combburst systems, while in starbursts this core is not seen until the third generation.

Since these systems exhibit similar intramolecular configurational behavior, it is quite reasonable to expect the configurationally dependent physical phenomena of combburst molecules to parallel that of their starburst analogues. The hydrodynamic characteristics (dependent on d_{app}) and intramolecular relaxation times (a consequence of intramolecular packing) of these systems are examples of such shared physical behavior. Since a double-logarithmic plot of $[\eta]$ versus M shows a maximum in intrinsic viscosity for starburst polymers,[4,8] a maximum will also be characteristic for combburst systems with $[\eta] \sim M^{-0.4}$ at high molecular weights. Note that the exponent of M can only be negative for systems having $d_{app} > 3$.[24] With regard to intramolecular relaxation, ^{13}C NMR performed on starburst molecules[4] confirms the existence of highly folded branches. Hence, similar ^{13}C NMR results are expected for combburst molecules. This testifies to the fact that the gross connectivity of starburst and combburst systems is the major determinant of their respective physical behavior on any length scale smaller than R_g but longer than l. Upon synthesis of combburst molecules, techniques mentioned, such as intrinsic viscosity measurements and ^{13}C NMR as well as neutron scattering (to determine the shape of the density profiles), will ultimately judge the validity of the conclusions drawn in the present study.

Throughout our discussion of the statistical properties of combbursts, we have refrained from establishing the existence of scaling laws. Rather, we characterize our systems by "power laws" having "apparent size exponents" for the following reasons. First, the structures generated in these studies will show $\rho \to 0, d_{app} \to \infty$ asymptotically.[25] This asymptotic regime is unattainable by using the KSAW algorithm to simulate this system. Hence, the stated value of ρ results from termination effects, which are algorithm and model dependent. Second, the inherent uncertainties in the off-lattice implementation of the KSAW, coupled with the relatively short chain lengths studied, may cause the exponents ρ and ν to have a systematic error approaching ±20%. Consequently, the molecular weights attainable in the present simulation lie within the crossover region of growth where scaling laws are not expected to exist. Despite the inability to reach the asymptotic regime, the density profiles and apparent exponents discussed here fully support the *qualitative* conclusions drawn in this study.

Acknowledgment. This work is supported by NSF Grant DMR-9008192. R.L.L. is grateful to K. G. Koniaris for writing the software used to generate Figure 2.

References and Notes

(1) Tomalia, D. A.; et al. *Macromolecules* **1986**, *19*, 2466.
(2) Tomalia, D. A.; Berry, V.; Hall, M.; Hedstrand, D. M. *Macromolecules* **1987**, *20*, 1167.
(3) Tomalia, D. A.; Naylor, A. M.; Goddard, W. A. *Angew. Chem., Int. Ed. Engl.* **1990**, *29*, 138.
(4) Meltzer, A. D. Ph.D. Thesis, University of Massachusetts, Amherst, 1990.
(5) Maciejewski, M. *J. Macromol. Sci., Chem.* **1982**, *A17* (4), 689.
(6) de Gennes, P.-G.; Hervet, H. *J. Phys. Lett.* **1983**, *44*, L351.
(7) Naylor, A. M.; Goddard, W. A. *Polym. Prepr.* (Am. Chem. Soc., Div. Polym. Chem.) **1988**, *29* (1), 215.
(8) Lescanec, R. L.; Muthukumar, M. *Macromolecules* **1990**, *23*, 2280.
(9) Zimm, B. H.; Stockmayer, W. H. *J. Chem. Phys.* **1949**, *17*, 1301.
(10) Stauffer, D. *Introduction to Percolation Theory*; Taylor and Francis: London, 1985.
(11) Stanley, H. E. *Introduction to Phase Transitions and Critical Phenomena*; OUP: Oxford, 1971.
(12) Flory, P. J. *J. Am. Chem. Soc.* **1941**, *63*, 3083.
(13) Stockmayer, W. H. *J. Chem. Phys.* **1943**, *11*, 45.
(14) Stockmayer, W. H. *J. Chem. Phys.* **1944**, *12*, 125.
(15) Vlahos, C. H.; Kosmas, M. K. *J. Phys. A: Math Gen.* **1987**, *20*, 1471.
(16) Lipson, J. E. G.; Gaunt, D. S.; Wilkinson, M. K.; Whittington, S. G. *Macromolecules* **1987**, *20*, 186.
(17) Majid, I.; Jan, N.; Coniglio, A.; Stanley, H. E. *Phys. Rev. Lett.* **1984**, *52* (15), 1257.
(18) Verdier, P. H.; Stockmayer, W. H. *J. Chem. Phys.* **1962**, *36*, 227.
(19) Baumgartner, A.; Binder, K. *J. Chem. Phys.* **1979**, *71*, 2541.
(20) Wall, F. T.; Mandel, F. *J. Chem. Phys.* **1975**, *63*, 4592.
(21) Kuhn, W. *Kolloid* 4Z. **1936**, *76*, 258.
(22) Peliti, L. *J. Phys. Lett.* **1984**, *45*, L925.
(23) Kremer, K.; Lyklema, J. W. *Phys. Rev. Lett.* **1985**, *55* (19), 2091.
(24) de Gennes, P.-G. *Scaling Concepts in Polymer Physics*; Cornell University: Ithaca, NY, 1979.
(25) Warner, M. Private communication.